Proc. 2001 Australian Conference on Robotics and Automation
Sydney, 14-15 November 2001

Autonomous Control of an Underground Mining Vehicle

Dr Peter Ridley
School of Mechanical Engineering,
Queensland University of Technology,
GPO Box 2434, Brisbane 4001, Australia,
p.ridley@qut.edu.au

Dr Peter Corke
CSIRO Manufacturing Science and Technology,
QCAT PO Box 883, Kenmore 4069,
Australia,
pic@cat.csiro.au

Abstract

This paper examines the kinematics and control of a Load Haul Dump Vehicle used in underground mining operations. The aim of the work is to develop an autonomous guidance strategy. A linear, state-space, mathematical model of the vehicle is derived purely from geometric consideration of the vehicle and its desired path. Autonomous regulation of the vehicle is shown to be theoretically feasible using state variable feedback of displacement, heading and curvature error. A relationship between stability and vehicle speed is derived. This expression forms the basis of an adaptive tuning strategy which optimises the vehicle's dynamic response.

1 Introduction

Load haul/dump (LHD) vehicles are used in underground metalliferous (non-coal) mining operations to retrieve and transport ore. Operation is cyclic, typically 15-18 trips per hour, with round trip distances from 100m to 600m. They are four-wheeled centre-articulated vehicles whose steering is achieved by control of the hitch joint angle. This kinematic structure creates a highly maneuverable vehicle, where the driver sits sideways in the middle of the vehicle. Changes from forward to reverse motion may be achieved without the driver changing posture. In dangerous mine locations these vehicles are steered by operators remote from the vehicle. The driver, who is often located in a control room, manually steers the vehicle using a joystick, with the view of the road coming via a video monitor. This mode of operation requires that vehicle speeds be lower than would be possible with the driver on board. Increases in vehicle speed and hence productivity may be made if the vehicle was capable of autonomous steering through the underground tunnels. Cunningham et al [1999] describe the benefits of underground vehicle automation.

2 Literature Review

Several authors have examined the theory of control of LHD vehicles. DeSantis [1997], Hemami and Polotski [1998] and Altafini [1999] are the most relevant to this paper. All four publications address the basic kinematic model of the vehicle and wrestle with the issue of how much control is necessary. They progress on the basis that path control is required over both the front and rear of the vehicle. This is a presumption we have not chosen, assuming instead that satisfactory control can be achieved by regulating the trajectory of a single point in the front of the vehicle. We contend that; providing slip between the wheels and the ground is negligible, and the hitch joint angle is specified, then the entire vehicle is constrained to follow a unique path. Scheding et al. [1997] suggest that slip is significant, however we believe that their analysis is incorrect because it is based on an inaccurate kinematic model of the vehicle. The same error is repeated by Steele et al reference [1997]. The no-slip kinematic model by Hemani and Polotski [1998] is also inaccurate. Both DeSantis [1997], and Altifini [1999] correctly identify the no slip-kinematic model of the LHD. This model is re-derived here using an alternative (relative velocity vector) method and is presented in equations (1) - (2) of this paper. Experimental evidence of the validity of this model is presented by Corke and Ridley [2000] who present data obtained from a 28 tonne LHD vehicle traveling over rough ground typical of a mine site.

Issues of path design are examined by Anderson et al. [1997] and Ishimoto et al. [1997]. This is a control strategy we have not used. Path design is associated with the guidance of a vehicle by steering it through a series of points whose absolute coordinates are known. This strategy is appropriate where the vehicle is required to navigate over a plane (or undulating) surface, where there is no intrinsically defined path. Guidance of farm machinery (Wilson [2000]), under a satellite Global Positioning System, is an ap-

plication where this strategy is necessary. Navigation of an LHD vehicle is different to these applications, not only because of its unique kinematic structure but also because of its unique underground environment. The vehicle will inevitably arrive at its destination provided it travels down the middle of the tunnel. Presence of tunnel walls makes that task of identifying the path relatively simple, compared with identifying a path along an open roadway, using conventional sensors. An autonomous LHD vehicle must be a regulator, which reacts purely to spurious path disturbance inputs, which include deviations in lateral displacement, heading and curvature of the vehicle's path compared with the path down the middle of the tunnel. Hemami and Polotski [1998] provide the genesis of this philosophy, but do not include extend their control strategy to cover second order path (curvature) control.

Scheding et al [1997] provide details of experimentation carried out using an instrumentation array mounted on a full-size test vehicle. They review "dead reckoning" sensors (encoders, inertial sensors, rate gyroscopes, accelerometers) capable of measuring vehicle motion and "external sensors" (laser and ultrasonic sensor) capable of measuring local path properties of the tunnel. In combination these transducers can identify errors in displacement, heading and curvature of the vehicle path compared with the tunnel path.

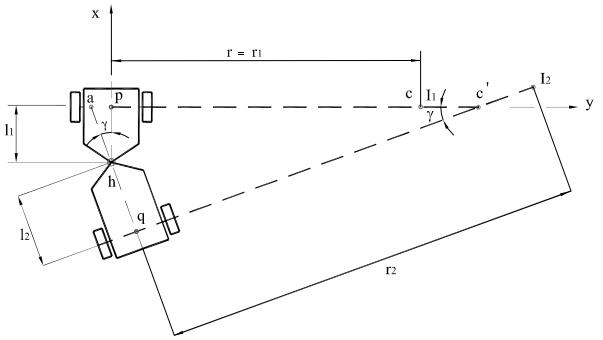

Figure 1: Geometric layout of LHD vehicle, showing the instantaneous centres (I_1 and I_2) of velocity of front and rear of the vehicle.

3 Vehicle Kinematics

Figure 1 shows a schematic plan view of the vehicle carrying a normal/tangential frame of reference whose origin coincides with p on the front axle midway between the wheels. The x-axis points forward, y-axis lies fixed along the front wheel axis and points to the starboard side of the vehicle and the z-axis is vertical downwards.

Lengths of the front and rear portions of the vehicle are designated l_1 and l_2 respectively. Steering angle γ is deemed positive when it causes the vehicle to turn clockwise. Forward speed of the vehicle is $v = V_p$, m/sec. Instantaneous centres of velocity of the front and rear are designated I_1 and I_2 respectively. The centre of curvature of the path of point p coincides with I_1 because the xy-frame is fixed to the front of the vehicle.

Assume that the vehicle is traveling forward without slip, with the steering angle changing at a rate $\dot{\gamma}$. Point h is common to both the front and rear of the vehicle,and velocities $V_p + V_{h/p} = V_q + V_{h/q}$. Since $\Omega_2 = \Omega_1 - \dot{\gamma}$, the relative velocity equation leads to a solution for the angular velocities of the front (Ω_1) and rear (Ω_2) of the vehicle ,

$$\Omega_1 = \frac{vsin\gamma + l_2\dot{\gamma}}{l_2 + l_1 cos\gamma} \ , \ \Omega_2 = \frac{vsin\gamma - l_1\dot{\gamma}}{l_2 + l_1 cos\gamma} \qquad (1)$$

Distance r_1 from p to the instantaneous centre of velocity I_1 of the front of the vehicle can also be determined,

$$r_1 = \frac{v}{\Omega_1} = v\left(\frac{l_2 + l_1 cos\gamma}{vsin\gamma + l_2\dot{\gamma}}\right). \qquad (2)$$

As noted previously, the instantaneous centre velocity of the front of the vehicle coincides with the centre of curvature of the path of point p. This coincident point is designated c in Figure 2, located at radius $r = r_1$ from point p along the x-axis.It is only when $\dot{\gamma} = 0$ that I_1,I_2 and c coalesce to a single point labeled c' in Figure 1.

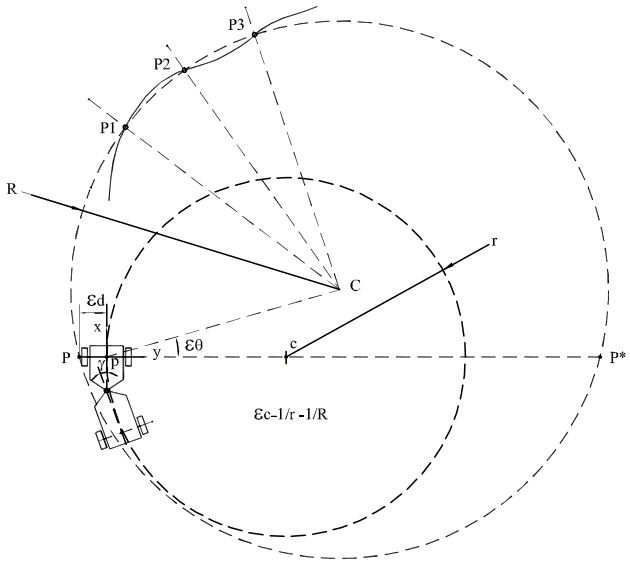

Figure 2: Plan-view of LHD vehicle, defining the displacement, heading and curvature errors (ϵ_d , ϵ_θ and ϵ_c) relative to the circle through points P_1, P_2 and P_3 on a prescribed path.

4 Vehicle path

Figure 2 shows a vehicle about to negotiate a path. Points P: (P_1,P_2,... etc) which lie on the desired path

may be used as targets for the vehicle trajectory. Circular interpolation requires that the point p on the vehicle should attempt pass through three nominated points P_1, P_2 and P_3 on the path. This would be achieved without any control action, if :

- point p in the vehicle initially coincides with any point (eg. P) on the desired path circle passing through points P_1, P_2 and P_3 and
- front wheel axle, y-axis, passes through the centre C of the desired path circle, and
- centre of curvature c of the vehicle path coincides with the centre C of the desired path circle.

A control strategy which automatically brings about these three conditions is examined in the following analysis.

Vehicle guidance requires a "look ahead" strategy to achieve accurate path tracking. Circular interpolation incorporates this feature by anticipating changes in path curvature, heading and position. The required look ahead distance will be determined by the speed of the vehicle and the latency in the steering actuator and may be adjusted by appropriate selection of points P_1, P_2 and P_3.

Vehicle forward speed (v) can be set by applying the strategy of keeping the normal acceleration (a_n) of the vehicle constant throughout the journey. If R is the radius of curvature of the desired path at a particular instant in the journey then, $v{=}\sqrt{a_n R}$. This speed control law reduces the vehicle speed on corners. Since the radius R is calculated from points ahead of the vehicle, it will decelerate prior to entering the bend and accelerate prior to leaving.

5 Equations of State

Figure 2 shows the initial state of the vehicle, at its approach to points P_1, P_2, P_3. Three variables:

- lateral displacement error,
- heading error and
- curvature error,

define the state of the vehicle relative to the circle, through these points. In order to obtain the desired circular path, steering inputs to the vehicle must be controlled in such a way as to reduce all three errors to zero. Positive errors in displacement, heading or curvature will be reduced through a reduction in hitch angle γ. Actual trajectory will be determined by the initial state of the vehicle and the vehicle kinematics.

The circle through points P_1, P_2 and P_3 intersects the y-axis twice at P and P^*, with point P being closer to p than P^*. Displacement error (ϵ_d) is the distance pP. Displacement error is positive when point P lies on the negative y-axis. If the circle does not intersect with the y-axis, then the displacement error is not defined. A different selection of points P_1, P_2 and P_3 , closer to the vehicle, is required. Heading error (ϵ_θ) is the angle between the line pC and the y-axis. An anticlockwise rotation of the vehicle is required to negate a positive heading error. Curvature error ($\epsilon_c = \frac{1}{r} - \frac{1}{R}$) measures the difference between the curvature of the desired path circle (R) and the curvature (r) of the path of point p in the vehicle. Radius (either R or r) is positive when the vehicle is undergoing a right-hand (clockwise) turn.

Figure 3 shows the point p moving to p' as a result of the vehicle moving $d\theta$ about its instantaneous centre c at radius r . Radial lines cp and Cp' intersect the desired path circle at P and P' respectively. The angle which defines the resulting progression of the vehicle about the circular path (centre C and radius R) lies between CP and CP' and is denoted $d\phi$.

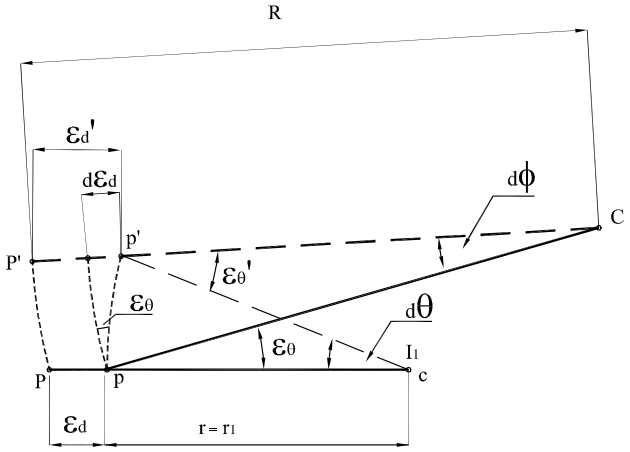

Figure 3: Geometric relationship between path errors (ϵ_d , ϵ_θ and ϵ_c) between two infinitesimally separated positions of the vehicle..

Assuming that both $d\theta$ and $d\phi$ are small angles measured in radians, then change in displacement error $d\epsilon_d = (rd\theta)\epsilon_\theta$. If this equation is divided throughout by dt and the substitution made that, $v = r\frac{d\theta}{dt}$, then

$$\dot{\epsilon}_d = v\epsilon_\theta. \tag{3}$$

Change in heading error $d\epsilon_\theta = d\theta - d\phi$. Since $(R - \epsilon_d)d\phi = rd\theta$, substitution for $d\phi$ from this equation gives $d\epsilon_\theta = d\theta\left(1 - \frac{r}{R-\epsilon_d}\right)$, which may be divided throughout by dt. Substituting for $\frac{d\theta}{dt}$ and assuming that $R >> \epsilon_d$, gives the expression

$$\dot{\epsilon}_\theta = v\epsilon_c + \dot{\gamma}\left(\frac{l_2}{l_2 + l_1 cos\gamma}\right). \tag{4}$$

Assuming that the vehicle speed v and desired path radius of curvature R are constant, the rate of change of curvature error, $\dot{\epsilon}_c = \frac{d\frac{1}{r}}{dt}$. From equation (2)

$$\frac{1}{r} = \frac{vsin\gamma + l_2\dot{\gamma}}{v(l_2 + l_1 cos\gamma)}, \tag{5}$$

differentiating this expression with respect to time gives,

$$\dot{\epsilon}_c = \frac{v(l_1 + l_2 cos\gamma)\dot{\gamma} + l_2(l_2 + l_1 cos\gamma)\ddot{\gamma} + (l_1 l_2 sin\gamma)\dot{\gamma}^2}{v(l_2 + l_1 cos\gamma)^2}. \quad (6)$$

The linearised state equation derived from the previous relationships (3), (4) and (6) is,

$$\begin{Bmatrix} \dot{\epsilon_d} \\ \dot{\epsilon_\theta} \\ \dot{\epsilon_c} \end{Bmatrix} = \begin{bmatrix} 0 & v & 0 \\ 0 & 0 & v \\ 0 & 0 & 0 \end{bmatrix} \begin{Bmatrix} \epsilon_d \\ \epsilon_\theta \\ \epsilon_c \end{Bmatrix} + \begin{Bmatrix} 0 \\ \frac{l_2}{L} \\ \frac{1}{L} \end{Bmatrix} \dot{\gamma} + \begin{Bmatrix} 0 \\ 0 \\ \frac{l_2}{vL} \end{Bmatrix} \ddot{\gamma} \quad (7)$$

The assumption has been made that γ is a small angle measured in radians and $L = l_1 + l_2$. Re-defining the third state variable allows us to put the state equation into a form containing a single input $\dot{\gamma}$. Substituting $\epsilon_c = \epsilon'_c + \frac{l_2}{vL}\dot{\gamma}$ gives

$$\begin{Bmatrix} \dot{\epsilon_d} \\ \dot{\epsilon_\theta} \\ \dot{\epsilon'_c} \end{Bmatrix} = \begin{bmatrix} 0 & v & 0 \\ 0 & 0 & v \\ 0 & 0 & 0 \end{bmatrix} \begin{Bmatrix} \epsilon_d \\ \epsilon_\theta \\ \epsilon'_c \end{Bmatrix} + \begin{Bmatrix} 0 \\ \frac{2l_2}{L} \\ \frac{1}{L} \end{Bmatrix} \dot{\gamma} \quad (8)$$

6 Control System Design and Analysis

Analysis of the state equation (8) shows that the state of the system is controllable using the input $\dot{\gamma}$. Assuming that all three of the state variables can be measured directly, automatic control of the path may be achieved using state variable feedback as shown in Figure 4. Full state feedback has the advantage, in theory,

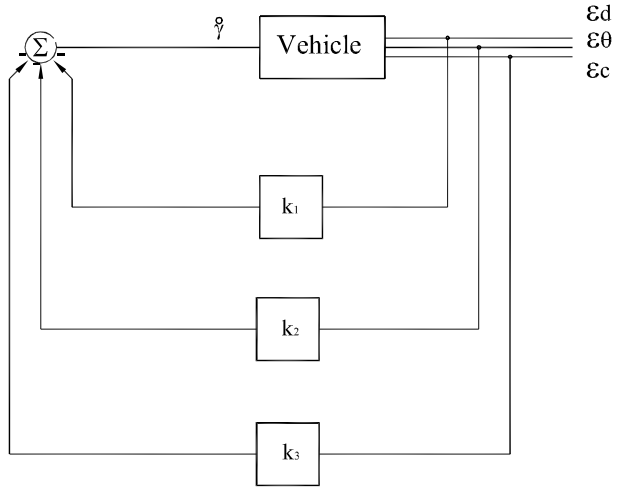

Figure 4: State variable feedback control strategy block diagram.

of allowing placement of the system's closed loop poles at any chosen location, in the S-plane. Hence we can tune the closed loop system to the specification of our choice. Suitable state feedback gains $[k_1, k_2, k_3]$ may be obtained which give the system a predominantly second order dynamic response with a prescribed natural frequency (ω_n) and damping ratio (ξ). The maximum practically attainable system natural frequency will be determined by the maximum slew rate attainable by the steering mechanism. A damping ratio of $\xi = 0.7$ gives minimum settling time. The third system pole may be rendered insignificant by placing it as far as possible to the left of the S-plane. The characteristic equation of the closed loop system is a third order polynomial whose coefficients are functions of vehicle size (l_2 and L) , speed (v) and the feedback gains $[k_1, k_2, k_3]$.

$$\ddot{\gamma}s^3 + \left(\frac{2l_2k_2 + k_3}{L}\right)s^2 + v\left(\frac{2l_2k_1 + k_2}{L}\right)s + v^2\left(\frac{k_1}{L}\right) = 0. \quad (9)$$

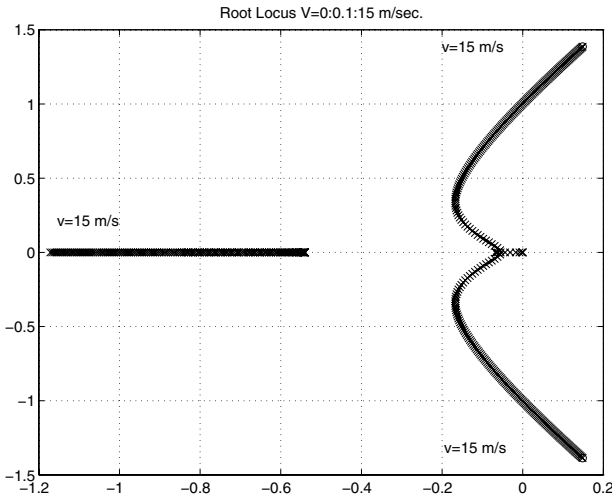

Figure 5: Locus of roots of the system characteristic equation as vehicle speed varies between zero and 15 m/s for constant feedback gains k = [0.0344,0.3536,1.6994].

Figure 5 shows the root locus of this polynomial as v changes. Increasing speed eventually leads to instability in steering if the feedback gains remain constant. It is desirable to maintain optimum tuning of the control system irrespective of vehicle speed. Coefficients of the characteristic equation can be kept constant by adaptively changing the feedback gains $[k_1, k_2, k_3]$, throughout the journey. Figure 6 shows how, for a particular pole placement, feedback gains must change with vehicle speed. Low speeds require large control effort to stabilise the vehicle; with control becoming impossible at zero speed. As speed increases, control effort derived from reaction to errors in displacement and heading approaches zero. Correction of the vehicle's path comes predominantly from the response to curvature error.

Consider the vehicle, shown in Figure 2, attempting to lock onto a prescribed path of constant curvature. Speed (v) remains constant.Feedback gains $[k_1, k_2, k_3]$ are tuned to provide a stable closed loop response. Errors [ϵ_d, ϵ_θ, ϵ_c] will decay to zero. Figures 7, 8 and 9 show a typical path response, by the vehicle. The Cartesian map of the vehicle path, relative to the cir-

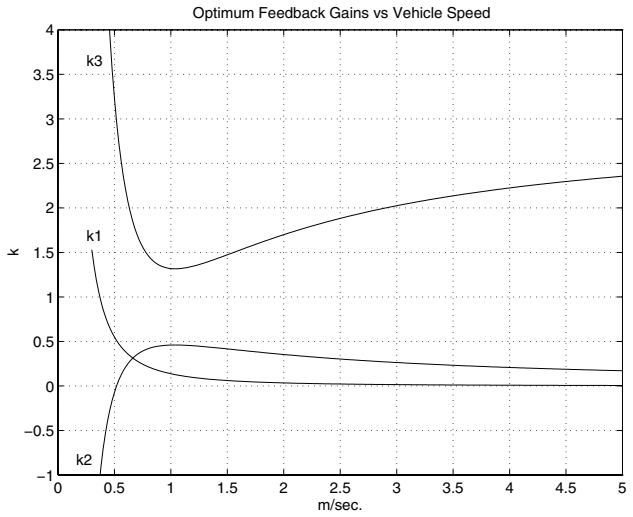

Figure 6: Variation of feedback gain required to maintain constant pole placement, ω_n =0.3 rad./sec. and ξ =0.7 , as vehicle speed varies. (l_1 =1.6, l_2 =1.8, R =10 m,)

cle, is shown in Figure 7. Notably, all three errors decay to zero as shown in Figure 8 and the steering angle γ reaches a steady state consistent with the radius R of the required circular path, as shown in Figure 9.

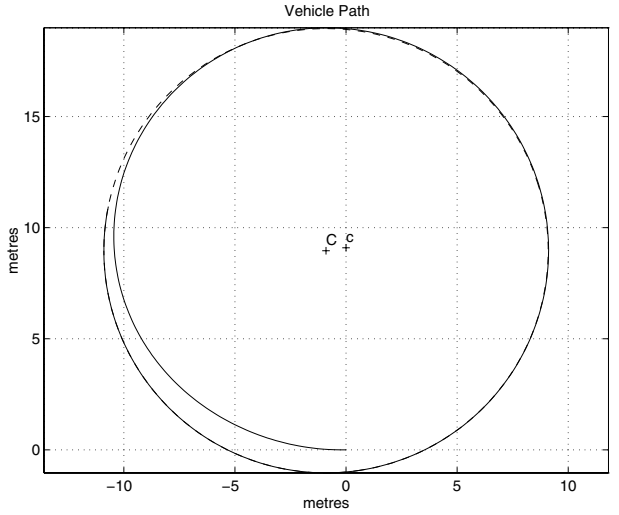

Figure 7: Path of an LHD vehicle as it locks onto a prescribed circle (R =10 m), from an initial position whose location errors are ϵ_d = 1.0 m, ϵ_θ= 0.1 rad. and ϵ_c = 0.0111m^{-1} . The vehicle speed is constant v= 2.0 m/sec. , and tuned (k = [0.0344,0.3536,1.6994]) for pole placement ω_n =0.3 rad./sec. and ξ =0.7 . (l_1 =1.6, l_2 =1.8)

7 Conclusion

The thesis of this paper is; that a vehicle traveling a complex (variable curvature) prescribed path under autonomous control should have its forward speed continuously regulated according to the local path curvature. In order to maintain invariant stability, the

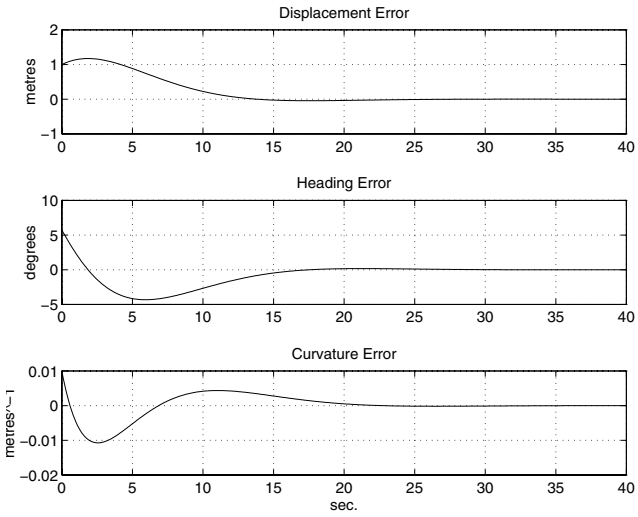

Figure 8: Error time response for the journey described in Figure 7.

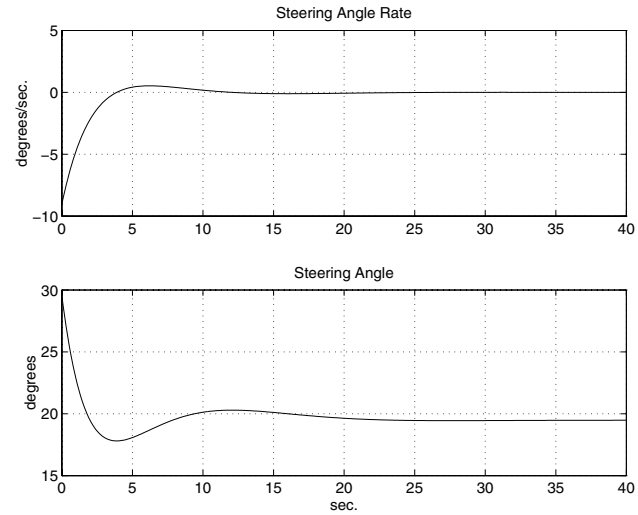

Figure 9: Steering time response for the journey described in Figure 7.

feedback gains need to be adaptively tuned to keep the coefficients of the characteristic equation constant. The navigation strategy is purely one of attempting to null a continuous set of disturbance input errors which confront the control loop.

The simple simulation using a linear kinematic model, has shown that autonomous control of the vehicle is theoretically feasible (except at very low speed). Further work currently being undertaken by the authors considers the application of this strategy on a full-size (28 tonne) LHD vehicle. Implications of the true non-linear nature of the system, including the latency in the steering dynamics still need to be addressed.

References

[Cunningham, *et al.*, 1999] , Cunningham, J. Corke, P., Durrant-Whyte, H. and Dalziel M. Automated LHDs and underground haulage trucks. *Australian Journal of Mining* Feb. 1999, pp51-53.

[DeSantis, 1997] DeSantis R. Modeling and path tracking for a load-haul-dump mining vehicle.*ASME Journal of Dynamic Systems, Measurement and Control*, Vol. 119, March 1997

[Hemami and Polotski, 1998] Hemami A., Polotski V., Path tracking control problem formulation of an LHD loader. *International Journal of Robotics Research*, Vol. 17, No. 2, February 1998, pp193-199.

[Altafini , 1999] Altafini C., A path-tracking criterion for an LHD articulated vehicle. *International Journal of Robotics Research*, Vol. 18, No. 5, May 1999, pp435-441.

[Altafini, 1999] Altafini C., Why use an articulated vehicle in mining operations. *Proceedings of the 1999 IEEE International Conference on Robotics and Automation*, Detroit, Michigan, May 1999 pp3020-3025

[Scheding *et al.,* 1997] Scheding S, Dissanayake G., Nebot E. Durrant-Whyte Slip modelling and aided inertial navigation of an LHD. Proceedings 1997 *IEEE Conference on Robotics and Automation*, April 20-25 1997, Albuquerque, New Mexico, pp1904-1909.

[Steele *et al.,* 1993], Steele J., Ganesh C., Kleve A. Control and scale model simulation of sensor-guided LHD mining machines. *IEEE Transactions on Industry and Applications*, Vol 29, No. 6 Nov./Dec. 1993 pp1232-1239

[Corke and Ridley, 2000] Corke P., Ridley P. Steering Kinematics for a Center-Articulated Mobile Robot. *IEEE Transactions on Robotics and Automation* [in press]

[Ishimoto *et al.,* 1997] Ishimoto H., Tsubouchi T., Sarata S. and Yuta S. A practical trajectory following of an articulated steering type vehicle. *Proceedings of the International Conference on Field and Service Robotics*, 8-10 December 1997, Canberra, pp412-419

[Andersson *et al.,*1997] Andersson U., Mrozek K., Hyyppa K., Astrom K. Path design and control algorithms for articulated mobile robots. *Proceedings of the International Conference on Field and Service Robotics*, 8-10 December 1997, Canberra, pp405-411

[Scheding *et al.,* 1997] Scheding S. Nebot E., Stevens M., Roberts J., Corke P., Cunningham J., Cook B. Experiments in Autonomous Underground Guidance. *Proceedings of the 1997 IEEE International Conference on Robotics and Automation*, Albuquerque, New Mexico, April 1997.

[Wilson, 2000] Wilson J. Guidance of agricultural vehicles. *Computers and Electronics in Agriculture*, Volume 25, Issues 1-2, January 2000, Pages 3-9